Title: Duplex functional G-quadruplex/NMM fluorescent probe for label-free detection of lead(II) and mercury(II) ions

Authors: Qian Zhu, Lanhua Liu, Yunpeng Xing, Xiaohong Zhou

PII: S0304-3894(18)30338-8
DOI: https://doi.org/10.1016/j.jhazmat.2018.04.082
Reference: HAZMAT 19365

To appear in: *Journal of Hazardous Materials*

Received date: 28-11-2017
Revised date: 17-4-2018
Accepted date: 30-4-2018

Please cite this article as: Zhu Q, Liu L, Xing Y, Zhou X, Duplex functional G-quadruplex/NMM fluorescent probe for label-free detection of lead(II) and mercury(II) ions, *Journal of Hazardous Materials* (2010), https://doi.org/10.1016/j.jhazmat.2018.04.082

Duplex functional G-quadruplex/NMM fluorescent probe for label-free detection of lead(II) and mercury(II) ions

Qian Zhu[1], Lanhua Liu[1], Yunpeng Xing[1, 2], Xiaohong Zhou[1]*

[1]State Key Joint Laboratory of Environmental Simulation and Pollution Control, Center for Sensor Technology of Environment and Health, School of Environment, Tsinghua University, Beijing 100084, China

[2]State Key Laboratory of Urban Water Resource and Environment, Harbin Institute of Technology, Harbin 150090, China

*xhzhou@mail.tsinghua.edu.cn

Graphical Abstract

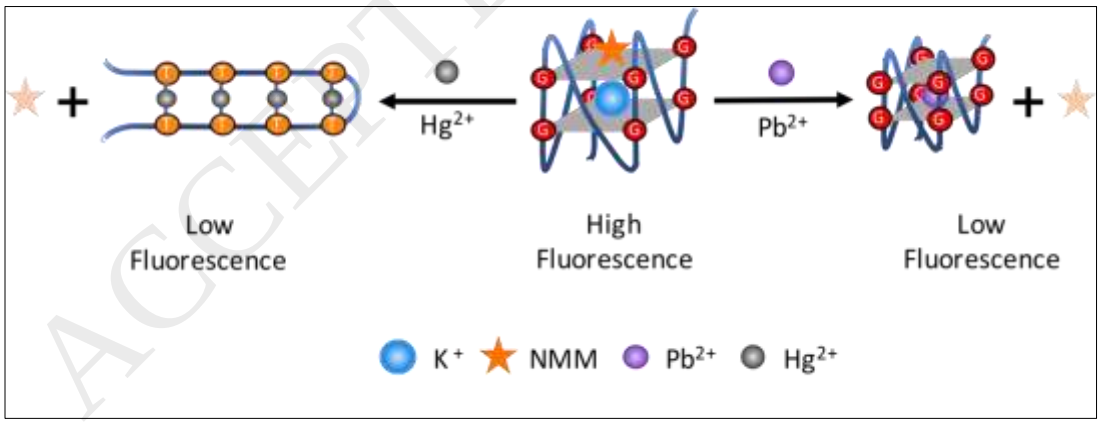

Highlights

1. A duplex functional fluorescent biosensor was established for the label-free and separate detection of Pb^{2+} and Hg^{2+}
2. The K^{+}-induced fluorescent G-quadruplex probe was assembled by a guanine-rich DNA sequence and N-methyl mesoporphyrin IX
3. Both Pb^{2+} and Hg^{2+} could cause the reassembly of DNA probe, consequently resulting in obvious fluorescence decrease
4. The method exhibited a low detection limit of 5.0 nM for Pb^{2+} and 18.6 nM for Hg^{2+}, respectively

Abstract: To meet the severe water pollution status, multi-target biosensor becomes one of research focus. We herein report a novel duplex functional fluorescent biosensor for the label-free and separate detection of Pb^{2+} and Hg^{2+} with high sensitivity and selectivity. A K^{+}-induced fluorescent G-quadruplex probe was assembled by a guanine-rich sequence (AGRO100) and N-methyl mesoporphyrin IX(NMM). It changed into a more stably non-fluorescent G-quadruplex structure and a hairpin-like structure upon binding Pb^{2+} and Hg^{2+} ions, respectively. As a result, the fluorescence decreased with relation to the addition of targets, allowing the separate detection of Pb^{2+} and Hg^{2+} ions at concentrations as low as 5 nM and 18.6 nM. The linear correlation existed between the fluorescence intensity and the concentration of

Pb^{2+} and Hg^{2+} over the range of 10 to 200 nM (R^2= 0.98) and 20 to 1000 nM (R^2= 0.99), respectively. All real lake samples, even containing Pb^{2+} or Hg^{2+} at 50 nM, could be determined by the duplex functional fluorescent probe with recovery rates 96% and 104%, respectively. Considering that this sensor is label-free, simple, time-saving, cost-effective and easy-to-handle, it is possible to pave its way for Pb^{2+} and Hg^{2+} detection in various application fields.

Keywords: Fluorescent DNA probe; N-methyl mesoporphyrin IX; G-quadruplex; Lead(II) ion; Mercury(II) ion

1 Introduction

Detection of heavy metal ions is of great importance because of their high toxicity and severe adverse effect on both environment and human health[1]. Lead and mercury are two of the most toxic metallic pollutants[2], thus the detection of them in environmental media, especially in aquatic media has caused worldwide concern. Traditional techniques to detect these two ions such as inductively coupled plasma mass spectrometry (ICP-MS) and atomic absorption spectrometry have been well developed and widely used[3-6], nevertheless, those techniques are expensive, complicated, and not suitable for on-site analyses.

Biosensors based on functional nucleic acids have been developed for the selective detection of Pb^{2+} and/or Hg^{2+} ions due to their rapid, simple, on-site, accurate and

low-cost advantages compared with the traditional chemical analysis[7]. For detection of lead ions, rationally designed G-quadruplex DNA probes have been extensively studied to realize a highly selective detection of Pb^{2+} in several decades[8-10]. G-quadruplexes are high-order structures formed from G-rich oligonucleotides through the stacking of planar G-tetrads[11-13]. In the presence of K^+, the guanine-rich sequences (e.g., PS2.M, AGRO100) form stable K^+-induced G-quadruplexes, which could bind to N-methyl mesoporphyrin IX (NMM) and cause enhanced fluorescence. NMM is an unsymmetrical anionic porphyrin with a pronounced structural selectivity for K^+-induced G-quadruplexes other than duplexes, triplexes, or single-stranded oligonucleotides[14]. The bound state of NMM would result in pronounced fluorescence enhancement compared with its free state, giving rise to specific detection of DNA G-quadruplex assembly and disassembly[15]. Pb^{2+} has been proved to competitively bind with K^+-induced G-quadruplexes due to the formation of more compact DNA folds[8, 16]. And Guo's work claimed that some Pb^{2+}-induced G-quadruplexes could show non-fit structures with NMM, hence leading to weak fluorescence[15]. For detection of Hg^{2+}, since the pioneering work by Ono and Togashi reported that mercury ions could bind in between two T-bases, promoting T–T mismatch[17], Over the past decade, various poly-T oligonucleotides based biosensors for Hg^{2+} using different signal transduction modes have been reported, including fluorescence[18, 19], colorimetry[20, 21], surface plasmon resonance[22, 23], surface-enhanced Raman scattering[24, 25] and electrochemistry[26, 27].

To meet the high demands of developing biosensors capable of multi-analyte detection

for heavy metal ions, many efforts have been taken over the years. However, although many previously reported biosensors realized to monitor Hg^{2+} or Pb^{2+}, a few of them could detect both kinds of metal ions simultaneously. Moreover, these duplex biosensor for detection of Hg^{2+} and Pb^{2+} still have some limitations such as high cost (e.g., Ti3C2 MXenes sensor[28]), needing complicated modifications (e.g., FAM and quencher labeling[29]). Although the label-free biosensors for the detection of Pb^{2+} and Hg^{2+} were in high demand due to their simplicity, rapidity and low cost, none such kind biosensors were reported to achieve sensitive and selective detection of Pb^{2+} and Hg^{2+}, simultaneously.

To circumvent these limitations, we herein reported a novel, facile technique for the selective and sensitive detection of Pb^{2+} and Hg^{2+}, separately, by using a DNA sequence called AGRO100 and NMM. The oligonucleotide AGRO100, which is originally selected as a potent anticancer aptamer[30], contains many T residues in addition to G residues with the ability to bind with Pb^{2+} or Hg^{2+} selectively. Inspired by this observation, we constructed a K^{+}-induced G-quadruplex/NMM complex, a fluorescent probe could be utilized as a turn-off sensor to detect Pb^{2+} and Hg^{2+} separately. The structure changes of the K^{+}-induced G-quadruplex/NMM fluorescent probe in the absence and presence of Pb^{2+} or Hg^{2+} were investigated by Circular Dichroism (CD). The experimental observations confirm the practicability of the quantitative analysis of aqueous Pb^{2+} or Hg^{2+} with high selectivity and sensitivity via this fluorescent biosensor.

2 Experimental

2.1 Chemicals and Instruments

Purified oligonucleotide AGRO100, d (GGTGGTGGTGGTTGTGGTGGTGGTGG), and purified oligonucleotide T20, d (TTTTTTTTTTTTTTTTTTTT), were obtained from Sangon Biotechnology Co., Ltd. (Shanghai, China). Acetic acid, 2,6-pyridinedicarboxylic acid (PDCA), N-methyl mesoporphyrin IX (NMM), Tris-(hydroxymethyl) aminomethane (Tris) and 19:1 acrylamide were bought from Sigma–Aldrich (USA). The used metal salts (KAc, $HgCl_2$, $Pb(Ac)_2$, $CdCl_2$, $CrCl_3$, $MgCl_2$, $CaCl_2$, $CoCl_2$, $ZnCl_2$, $NiCl_2$, $FeCl_3$ and $CuCl_2$) were obtained from Beijing Chemical Reagent Company (Beijing, China). SYBR® Gold Nucleic Acid Gel stain was purchased from Thermo Fisher Scientific (USA). All other chemicals were of analytical grade. All reagents were used as received without further purification. Before use, the stock solution of NMM (1 mM) was prepared in ultrapure water and stored in the dark at -20 °C, and diluted to the required concentrations with Tris–HAc buffer (10 mM, 20 mM KAc, pH 7.4).

Before use, the stock solution of AGRO100 was prepared by DNase- and RNase-free water and quantified by using UV-vis absorption spectroscopy with the following extinction coefficients ($\varepsilon_{260\ nm}$, $M^{-1}\ cm^{-1}$): A=15400, G=11500, C=7400, T=8700. Before fluorescent measurement, the AGRO100 stock solution was heated at 88 °C for 10 min and gradually cooled down to room temperature. 500 μL AGRO100 stock solution of 10 μM was firstly prepared in Tris–HAc buffer (10 mM, 20 mM KAc, pH

7.4).

A HITACHI F-7000 fluorescence spectrophotometer was used to record the fluorescence intensity. The optical chamber (1 cm path length, 0.35 mL volume) was deoxygenated with dry purified nitrogen (99.99 %) before use. Circular Dichroism (CD) was conducted using a by a Chirascan^{TM} circular dichroism spectrometer (Applied Photophysics, UK). A gel imaging system Doc XR (BioRad, America) was used to record the image of DNA bands.

2.2 Circular Dichroism and Non-denaturing PAGE

Circular Dichroism. A quartz cuvette with a 1-mm path length was used for the spectra recorded over wavelengths ranging from 230 nm to 320 nm at 1 nm bandwidth, 1 nm step size, and 0.5 s per point. 10 mM Tris-HAc buffer (pH 7.4) was applied to make blank corrections before measurement. All samples were prepared with 20 μM AGRO100 in 10 mM Tris-HAc buffer (pH 7.4) and incubated 20 min at room temperature. Moreover, the spectra were monitored at different temperatures at 260 nm to determine the melting temperature (T_m) with the control wavelength of 320 nm. The temperature gradient was 1°C/min between 10°C and 90°C.

Non-denaturing PAGE. All samples were prepared with 4 μM AGRO100 in 10 mM Tris-HAc buffer (pH 7.4) and incubated 20 min at room temperature. Non-denaturing 20% PAGE was run in 1× TBE buffer at 100 Vcm^{-1} and 4°C for 4 h, then the gel was stained with 3× SYBR® Gold Nucleic Acid Gel Stain for 30 min for PAGE imaging.

2.3 Analysis of Samples

Sensitivity. For Pb^{2+} testing, Pb^{2+} at various concentrations was introduced into 200 μL aliquots of Tris–HAc buffer (10 mM, 20 mM KAc, pH 7.4), containing 1 μM AGRO100. After incubated 20 min at room temperature, 4.6 μL NMM of 100 μM was added into each sample. After incubation, samples were kept in darkness at room temperature for 15 min, and then the fluorescence intensity of each sample was monitored. For Hg^{2+} testing, the similar procedures were carried out except that Pb^{2+} were replaced by Hg^{2+}.

Selectivity. To investigate the selectivity, different nonspecific metal ions, including 100 μM Ca^{2+}, 100 μM Mg^{2+}, 10 μM Mn^{2+}, 10 μM Fe^{3+}, 1 μM Cd^{2+}, 1 μM Cr^{2+}, 1 μM Co^{2+}, 1 μM Zn^{2+}, 1 μM Ni^{2+} and 1 μM Cu^{2+}, were added into the sensing solution individually and the differences in the fluorescence intensity were analyzed. Quenching efficiency ($(I_0-I)/I_0$) of the fluorescence intensity at wavelength of 610 nm was selected as an index to indicate the selectivity.

Environmental samples. Real water samples from Hetang Lake (Beijing, China) were selected to demonstrate the practicability of this developed biosensor. The water samples were filtered through a 0.22 μm filter and adjusted to pH 7.4 before analysis. To improve accuracy, all measurements were performed in triplicate.

3 Results and discussion

3.1 Sensing mechanism

The sensing strategy of duplex functional K^+-induced G-quadruplex/NMM complex fluorescent probe toward the detection of Pb^{2+} and Hg^{2+} ions is demonstrated in **Scheme 1**. The AGRO100 has been reported to have a random coil structure that could fold into a G-quartet structure in the presence of a very small amount of K^+ ions[31, 32]. The K^+-induced G-quadruplexes bound to NMM, giving arise to high fluorescence. When the Pb^{2+} ions were added into the system, considering the Pb^{2+}-induced G-quadruplexes were more stable than K^+ ones[8, 16], the reassembly of Pb^{2+}-induced G-quadruplexes occurred, which showed little interaction with NMM[2, 6, 15], leading to decreased fluorescence. Alternatively, with the addition of Hg^{2+} to the sensing system, the T residues of the AGRO100 probe could bind to Hg^{2+} ions through T-Hg^{2+}-T interaction. It induced the formation of a hairpin-like structure, causing a decrease in fluorescence as similar as the addition of Pb^{2+}.

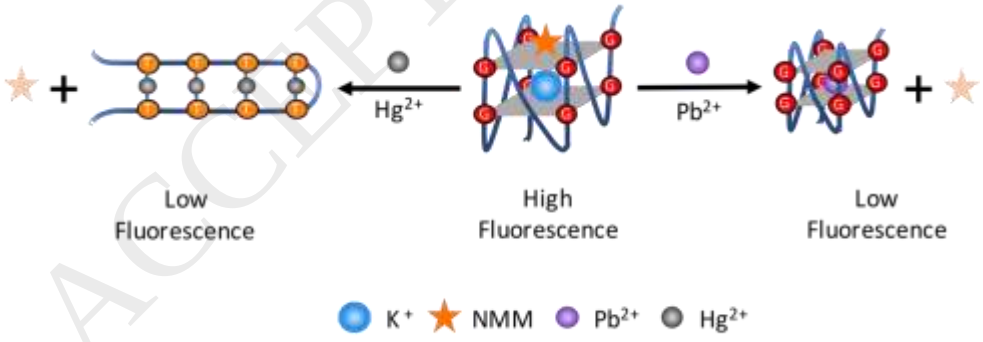

Scheme 1 Cartoon schematic of K^+-induced G-quadruplex/NMM complex fluorescent probe utilizing AGRO100 and NMM for label-free and facile detection of Hg^{2+} and Pb^{2+}, separately

Proof-of-concept experiments were carried out to confirm the above proposed principle. As shown in **Figure 1**, the pure NMM displayed almost no fluorescence (curve **a**), while after the interaction with AGRO100 probe and K^+, the fluorescence was greatly enhanced (curve **b**). As expected, the fluorescence was decreased to different degrees upon addition of Hg^{2+} (500 nM) or Pb^{2+} (100 nM), as curves **c** and **d** indicated, respectively.

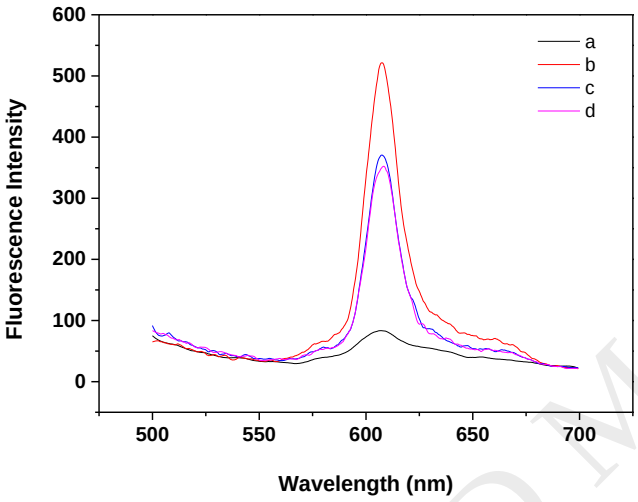

Figure 1 Fluorescence emission spectra. **a.** 2.3 μM NMM **b.** 1 μM AGRO100, 2.3 μM NMM. **c.** 500 nM Hg^{2+}. **d.** 100 nM Pb^{2+}. All samples were prepared in 200 μL Tris–HAc buffer (10 mM, 20 mM KAc, pH 7.4)

3.2 Characterization of AGRO100 structure by CD and PAGE

To characterize the structure of different G-quadruplexes, several techniques, including Circular Dichroism (CD), Gel Electrophoresis, Electrospray Mass Spectrometry, Thermal Denaturation, have been developed in recent years[33-36]. In this work, CD spectra and non-denaturing Polyacrylamide Gel Electrophoresis

(non-denaturing PAGE) experiments were carried out to investigate the structures of AGRO100.

The CD spectra were obtained to provide the experimental evidence of formation of K^+-induced G-quadruplexes and its structure changes in presence of Pb^{2+} or Hg^{2+}. **Figure 2** shows the CD spectra of AGRO100 structure influenced by metal ions. The CD spectra of AGRO100 without salt exhibited a weak absorption (**curve a**) showing that few secondary structures existed. In the presence of K^+ ions, a high positive peak at λ = 260 nm and a weak positive band at λ = 290 nm were observed due to the form of of a parallel G-quadruplex structure induced by K^+ ions, in agreement with previous reports[33, 34, 36, 37] (**curve b**). After the addition of Hg^{2+}, there was a decrease in the height and the amplitude of the positive peaks of K^+-induced G-quadruplexes (**curve c**), indicating a change of DNA structure. By contrast, the addition of Pb^{2+} made no significant difference (**curve d**), indicating the possibility that G-quadruplexes induced by K^+ and Pb^{2+} were parallel structure, respectively, which could not be distinguished by CD spectra.

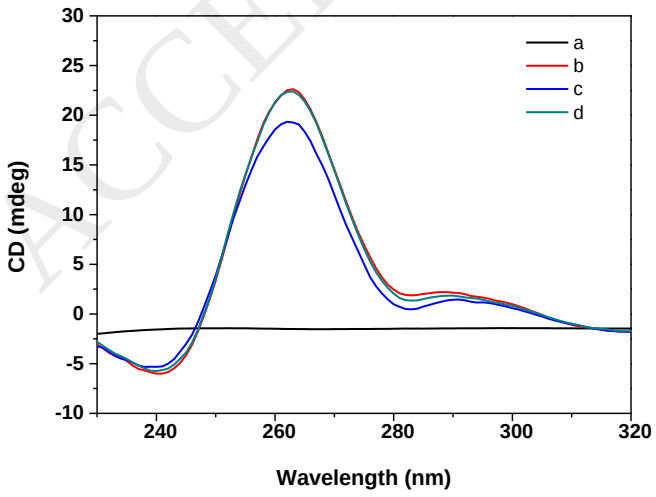

Figure 2 CD spectra of AGRO100 structure. **a.** No salt. **b.** 400 mM K^+. **c.** 400 mM K^+, 40 μM Hg^{2+}. **d.** 400 mM K^+, 40 μM Pb^{2+}. All samples included 20 μM AGRO100 in 10 mM Tris-HAc buffer (pH 7.4)

For further characterization of G-quadruplex topologies, the non-denaturing PAGE was conducted. **Figure 3** shows the results of non-denaturing PAGE for AGRO100 in 10 mM Tris–HAc buffer (pH 7.4) at 4°C. The PAGE experiment was obtained at low temperature as 4°C to avoid potential change of DNA structure during electrophoresis. In native conditions, the migration of single-stranded oligonucleotides (**Lane 2** and **Lane 3**) was faster than 20-base pair duplex of 40 bases (Lane 1). Two different bands were observed in **Lane 4**, probably indicating that G-quadruplexes formed in the presence of K^+. Considering the G-quadruplex structure migrated slower than the single-stranded DNA with same sequence, combined with the results of CD spectra, it is reasonable to assume that K^+-induced G-quadruplex corresponded to an intramolecular parallel G-quadruplex[33].

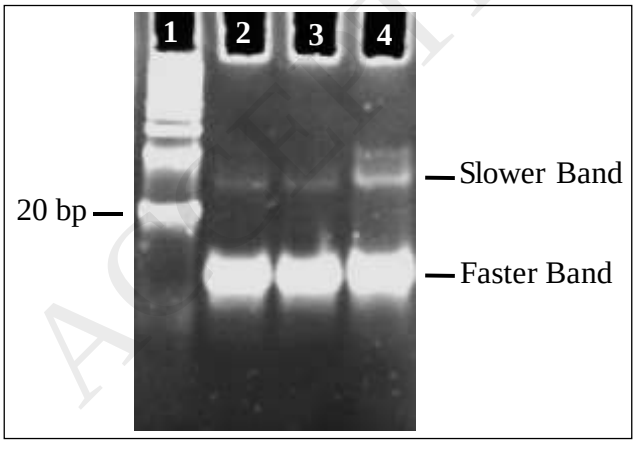

Figure 3 Non-denaturing 20% PAGE image of AGRO100 (4 μM) in 10 mM Tris–HAc buffer (pH 7.4) at 4°C. (**Lane 1**, Marker; **Lane 2** and **Lane 3**, no K^+ ions; **Lane 4**, 160

mM K^+)

To further illustrate the structure changes of AGRO100 in the presence of Hg^{2+} or Pb^{2+}, the thermal denaturation experiments were further conducted. As **Figure 2** shows, the CD spectra of K^+-induced G-quadruplexes had a high positive peak at $\lambda = 260$ nm. Therefore, CD at 260 nm was monitored from 10 °C to 90 °C, and T_m was calculated as Marky described[38]. **Figure 4** shows the melting curves of AGRO100 with metal ions. In the presence of K^+ ions, oligonucleotides formed stable G-quadruplex structure (**curve a**), and the T_m value of K^+-induced G-quadruplexes is 77°C. When Pb^{2+} or Hg^{2+} ions were added, the characteristic peak of K^+-induced G-quadruplexes at 260 nm performed weaker CD signal and lower T_m (64°C for **curve b** and 64°C for **curve c**). The results prove that Pb^{2+} or Hg^{2+} ions could destroy K^+-induced G-quadruplexes and form other stable structures instead, indicating the practicability of the mechanism shown in **Scheme 1**.

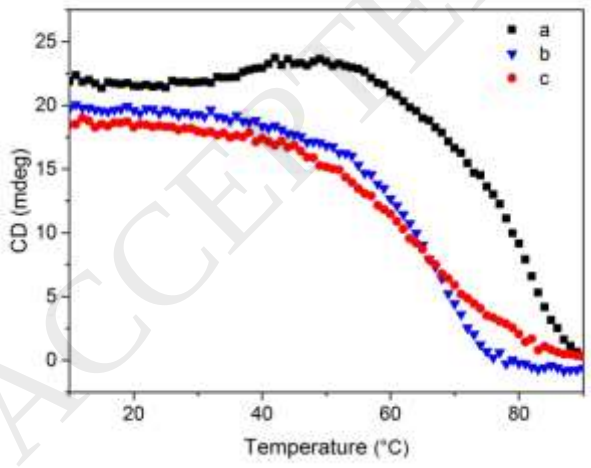

Figure 4 CD melting curves for AGRO100 monitored at 260 nm. **a.** 400 mM K^+. **b.** 400 mM K^+, 100 μM Pb^{2+}. **c.** 400 mM K^+, 100 μM Hg^{2+}. All samples included 20 μM AGRO100 in 10 mM Tris-HAc buffer (pH 7.4)

3.3 Sensitivity

Under the optimized conditions (see **Figure S1 and S2**), the sensitivities of the established method towards Pb^{2+} and Hg^{2+} were investigated individually. As expected, the fluorescence intensities decreased with the increased concentrations of Pb^{2+} (**Figures 5a** and **5b**) or Hg^{2+} (**Figures 5c** and **5d**). The insets in **Figures 5b** and **5d** show the linear responses of fluorescence against the concentrations of Pb^{2+} and Hg^{2+} over the ranges from 10 nM to 200 nM ($R^2 = 0.98$) and 20 nM to 1000 nM ($R^2 = 0.99$), respectively. The limits of detection (LoDs, based on $3\sigma/\text{slope}$ rule) are 5.0 nM for Pb^{2+} and 18.6 nM for Hg^{2+}. As illustrated in **Table 1**, relative to other Pb^{2+} and/or Hg^{2+} sensors, this biosensor showed better or comparable sensitivity. According to the World Health Organization (WHO) defined toxicity level of Hg^{2+} (30 nM) and Pb^{2+} (48 nM) in drinking water[39], the established biosensor could be enough sensitive to monitor the Pb^{2+} or Hg^{2+} contaminants for the requirement of drinking water standard.

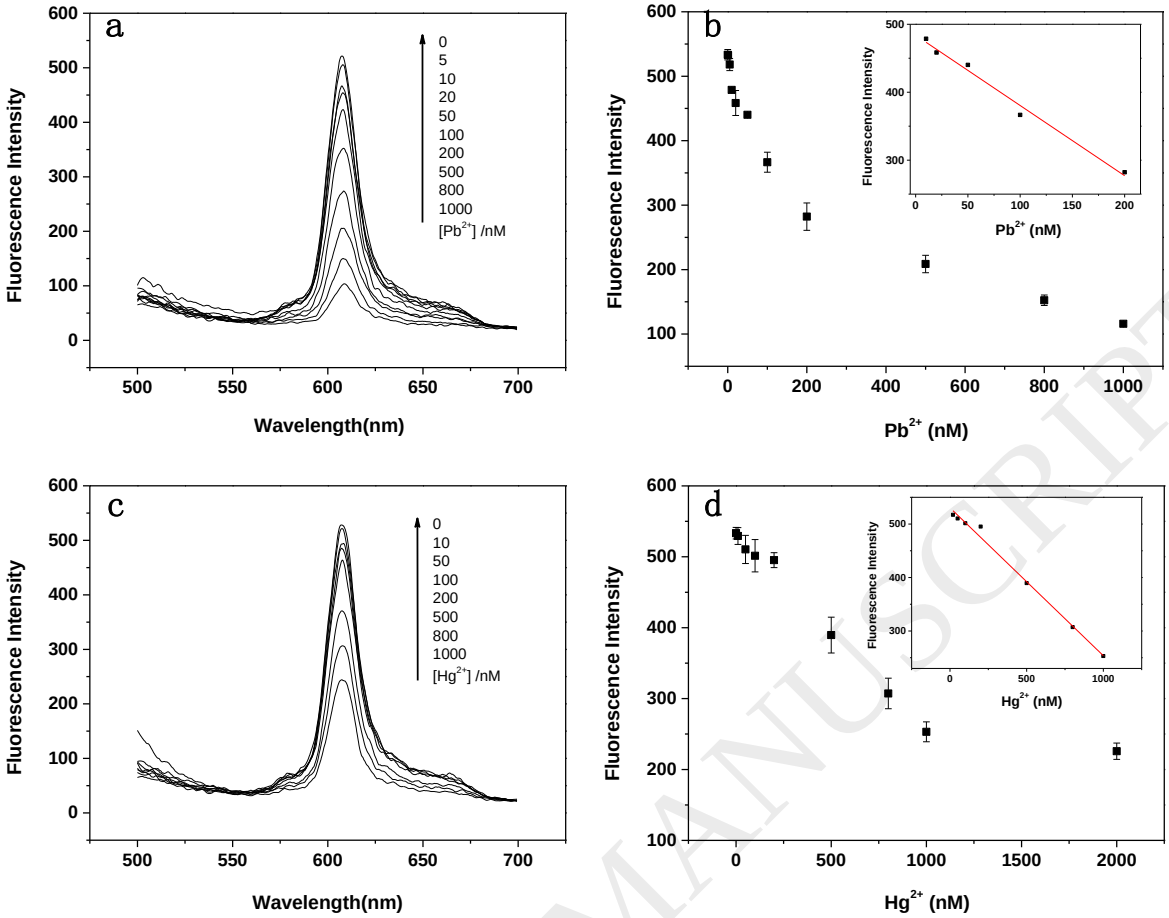

Figure 5 Sensitivity for detection of aqueous Pb^{2+} or Hg^{2+} ions. **a.** Fluorescence emission spectra of Pb^{2+} ions concentration (0, 5, 10, 20, 50, 100, 200, 500, 800, 1000 nM). **b.** Fluorescence intensity at wavelength of 610 nm with respect to the Pb^{2+} ions concentrations used in **a**. The inset shows the linear relationship over the concentration range from 10 to 200 nM. **c.** Fluorescence emission spectra of Hg^{2+} ions concentration (0, 10, 20, 50, 100, 200, 500, 800, 1000 nM). **d.** Fluorescence intensity at wavelength of 610 nm with respect to the Hg^{2+} ions concentrations used in **c**. The inset shows the linear relationship between the fluorescence and the concentration of Hg^{2+} over the range from 20 to 1000 nM.

Table 1 Comparison of the sensitivities using different Pb^{2+} and/or Hg^{2+} sensors

Methods	Target	LOD	Linear range	Reference
Fluorescence	Pb^{2+}	20 nM	20 nM-1 μM	[10]
	Hg^{2+}	40 nM	40 nM-100 nM	[17]
	Pb^{2+}	0.3 nM	0.5-30 nM	[29]
	Hg^{2+}	5 nM	10-200 nM	
Colorimetry	Hg^{2+}	8 nM	10 nM-5 μM	[20]
Electrochemistry	Pb^{2+}	41 nM	100 nM-550 nM	[28]
	Hg^{2+}	130 nM	1.0 μM-1.9 μM	
Label-free	Pb^{2+}	5 nM	10 nM-200 nM	This study
	Hg^{2+}	18.6 nM	20 nM-1000 nM	
	Pb^{2+}	1 nM	5.0 nM-1.0 μM	[15]
	Hg^{2+}	15 nM	50 nM-300 nM	[21]

3.4 Selectivity

The selectivity of the sensing system for Hg^{2+} or Pb^{2+} detection was evaluated by using other environmentally relevant metal ions instead of targets, including Ca^{2+}, Mg^{2+}, Mn^{2+}, Fe^{3+}, Cd^{2+}, Cr^{2+}, Co^{2+}, Zn^{2+}, Ni^{2+} and Cu^{2+} under the same conditions, respectively.

To overcome the interference from Pb^{2+} in Hg^{2+} detection, 2,6-pyridinedicarboxylic acid (PDCA) was introduced as the masking agent. PDCA has been reported as an effective chelating agent able to strongly complex with Pb^{2+} in aqueous solutions[40, 41]. Thus, PDCA was selected to improve the selectivity for Hg^{2+} detection. As shown

in **Figure 6**, in the selectivity trials, 200 nM Pb^{2+} or 1 μM Hg^{2+} significantly changed the fluorescence intensity, the quenching efficiency was about 0.5. By contrast, other competing ions (including 100 μM Ca^{2+}, 100 μM Mg^{2+}, 10 μM Mn^{2+}, 10 μM Fe^{3+}, 1 μM Cd^{2+}, 1 μM Cr^{2+}, 1 μM Co^{2+}, 1 μM Zn^{2+}, 1 μM Ni^{2+} and 1 μM Cu^{2+}) caused virtually no positive change in the quenching efficiency. These results suggest that the developed biosensor for Pb^{2+} and Hg^{2+} displayed a highly favorable and specific recognition comparable with competing ions, indicating high selectivity of Pb^{2+} and Hg^{2+}, respectively. **Figure 6** shows that no interference from Pb^{2+} was found in the presence of PDCA. To overcome the interference from Hg^{2+} in Pb^{2+}detection, T20 sequence was selected as a masking agent. Considering the T–Hg^{2+}-T mismatch[17], this oligonucleotides with 20 T residues could competitively bind to Hg^{2+} and form more stable structure. The concentration of T20 added to samples was studied (see **Figure S3**), and **Figure 6** shows that no interference from Hg^{2+} was found in the presence of 500 nM T20, demonstrating that Pb^{2+} and Hg^{2+} could be detected and distinguished by this biosensor.

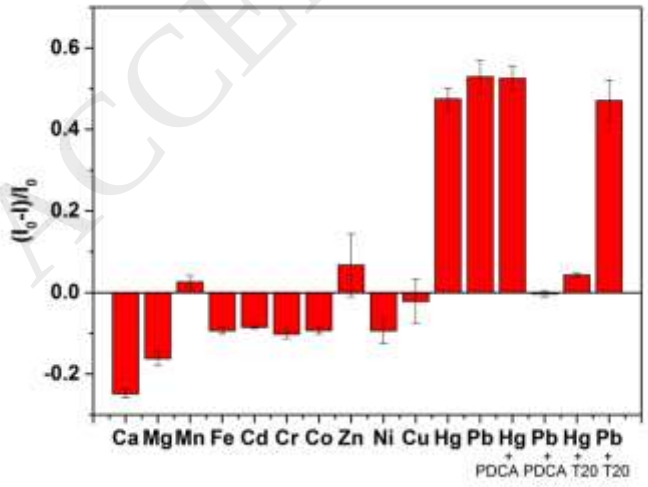

Figure 6 Quenching efficiency ($(I_0-I)/I_0$) of the fluorescence intensity at wavelength of 610 nm in the presence of individual metal ion. All tested metal ions were 100 μM Ca^{2+}, 100 μM Mg^{2+}, 10 μM Mn^{2+}, 10 μM Fe^{3+}, 1 μM Cd^{2+}, 1 μM Cr^{2+}, 1 μM Co^{2+}, 1 μM Zn^{2+}, 1 μM Ni^{2+}, 1 μM Cu^{2+}, 1 μM Hg^{2+}, 200 nM Pb^{2+}, 1 μM Hg^{2+} with 20 μM PDCA, 200 nM Pb^{2+} with 20 μM PDCA, 1 μM Hg^{2+} with 500 nM T20, 200 nM Pb^{2+} with 500 nM T20. Other experimental conditions were equal to those shown in **Figure 1 b**.

3.5 Recovery Study

The recovery study of this biosensor was performed in real lake water samples from Hetang Lake at Tsinghua University campus, spiked with or without Pb^{2+} or Hg^{2+} (0, 50 nM), respectively. All water samples were filtered by a 0.22 μm filter before measurement. The concentrations measured were compared with those added and results are exhibited in **Table 2**. The biosensor showed no significant signal change when the non-spiked samples were added, indicating that Pb^{2+} and Hg^{2+} were not present in these samples. The average recoveries of Pb^{2+} (96% ± 12%) and Hg^{2+} (104% ± 7%) demonstrated the satisfactory accuracy of the biosensor and indicated the application potential in real water samples.

Table 2 Recovery study in spiked lake water samples

Sample	**Found (nM)**	**Spiked (nM)**	**Recovered (nM)**	**Recovery (%)**	**RSD (%)**
Lake water	not detected	50 nM Pb^{2+}	47.8	96	12

	50 nM Hg^{2+}	51.8	104	7

4. Conclusion

In summary, we demonstrated a novel, duplex functional fluorescent biosensor for the facile detection of lead(II) or mercury(II) with high sensitivity and selectivity. The LoDs of this method were as low as 5.0 nM for Pb^{2+} and 18.6 nM for Hg^{2+}, respectively. Compared with previous studies, the established method is label-free, cost-effective, time-effective, simple and easy-to-handle. Considering that real lake samples containing Pb^{2+} or Hg^{2+} at 50 nM were determined by the biosensor with recovery rates 96% and 104%, this biosensor could be applied in the practical measurement of Pb^{2+} or Hg^{2+} in real water samples.

Acknowledgement

This work was supported by Tsinghua University Initiative Scientific Research Program (20161080166) and Tsinghua University's Challenge Based Learning course construction project DX02_11.

References

[1] S. Bent, C. Göttsch, U. Braam, W. Schmutzler, The effects of heavy metal ions (Cd^{2+}, Hg^{2+}, Pb^{2+}, Bi^{3+}) on histamine release from human adenoidal and cutaneous mast cells, Agents & Actions, 36 (1992) C321-C324.

[2] F.C. Vincent, C.R.B. Blackburn, The effects of heavy metal ions on the human

erythrocyte i. comparisons of the action of several heavy metals, Australian Journal of Experimental Biology & Medical Science, (1958).

[3] W.R. Hatch, W.L. Ott, Determination of submicrogram quantities of mercury by atomic absorption spectrophotometry, Anal Chem, 40 (1968) 2085.

[4] V. Lagesson, L. Andrasko, Direct determination of lead and cadmium in blood and urine by flameless atomic absorption spectrophotometry, Clin Chem, 25 (1979) 1948-1953.

[5] A. Schütz, I.A. Bergdahl, A. Ekholm, S. Skerfving, Measurement by ICP-MS of lead in plasma and whole blood of lead workers and controls, Occupational & Environmental Medicine, 53 (1996) 736.

[6] Y. Li, C. Chen, B. Li, J. Sun, J. Wang, Y. Gao, Y. Zhao, Z. Chai, Elimination efficiency of different reagents for the memory effect of mercury using ICP-MS, J Anal At Spectrom, 21 (2005) 94-96.

[7] J. Liu, Z. Cao, Y. Lu, Functional Nucleic Acid Sensors, Chem Rev, 109 (2009) 1948-1998.

[8] F.W. Kotch, J.C. Fettinger, J.T. Davis, A lead-filled G-quadruplex: insight into the G-Quartet's selectivity for Pb(2+) over K(+), Org Lett, 2 (2000) 3277.

[9] I. Smirnov, R.H. Shafer, Lead is unusually effective in sequence-specific folding of DNA, J Mol Biol, 296 (2000) 1.

[10] T. Li, S. Dong, E. Wang, A Lead(II)-Driven DNA Molecular Device for Turn-On Fluorescence Detection of Lead(II) Ion with High Selectivity and Sensitivity, J Am Chem Soc, 132 (2010) 13156-13157.

[11] H.J. Lipps, D. Rhodes, G-quadruplex structures: in vivo evidence and function, Trends Cell Biol, 19 (2009) 414.

[12] T. Simonsson, G-quadruplex DNA structures--variations on a theme, Biol Chem, 382 (2001) 621.

[13] J.T. Davis, G-quartets 40 years later: from 5'-GMP to molecular biology and supramolecular chemistry, Angewandte Chemie International Edition, 43 (2004) 668-698.

[14] L. Ma, H. Liu, G. Wu, N. Sun, L. Meng, Y. Li, Z. Liu, A. Diao, A dual-channel detection of mercuric ions using a label free G-quadruplex-based DNAzyme molecule, Analyst, 141 (2016) 3997.

[15] L. Guo, D. Nie, C. Qiu, Q. Zheng, H. Wu, P. Ye, Y. Hao, F. Fu, G. Chen, A G-quadruplex based label-free fluorescent biosensor for lead ion, Biosens Bioelectron, 35 (2012) 123-127.

[16] T. Li, E. Wang, S. Dong, Potassium-lead-switched G-quadruplexes: a new class of DNA logic gates, J Am Chem Soc, 131 (2009) 15082.

[17] A. Ono, H. Togashi, Highly selective oligonucleotide-based sensor for mercury(II) in aqueous solutions, Angewandte Chemie, 43 (2004) 4300.

[18] Z. Wang, J.H. Lee, Y. Lu, Highly sensitive “turn-on” fluorescent sensor for Hg2+ in aqueous solution based on structure-switching DNA, Chemical Communications, 45 (2008) 6005.

[19] R. Wang, X. Zhou, H. Shi, Y. Luo, T-T mismatch-driven biosensor using triple functional DNA-protein conjugates for facile detection of Hg(2.), Biosens Bioelectron,

78 (2016) 418-422.

[20] Y. Zhou, H. Dong, L. Liu, M. Li, K. Xiao, M. Xu, Selective and sensitive colorimetric sensor of mercury (II) based on gold nanoparticles and 4-mercaptophenylboronic acid, Sensors & Actuators B Chemical, 196 (2014) 106-111.

[21] A.G. Memon, X. Zhou, J. Liu, R. Wang, L. Liu, B. Yu, M. He, H. Shi, Utilization of unmodified gold nanoparticles for label-free detection of mercury (II): Insight into rational design of mercury-specific oligonucleotides, J Hazard Mater, 321 (2017) 417-423.

[22] L. Wang, T. Li, Y. Du, C. Chen, B. Li, M. Zhou, S. Dong, Au NPs-enhanced surface plasmon resonance for sensitive detection of mercury(II) ions, Biosens Bioelectron, 25 (2010) 2622.

[23] J. Castillo, J. Chirinos, H. Gutiérrez, M.L. Cruz, Surface plasmon resonance sensor based on golden nanoparticles and cold vapour generation technique for the detection of mercury in aqueous samples, Optics & Laser Technology, 94 (2017) 34-39.

[24] G.Q. Wang, L. Chaesung, L.X. Chen, C. Hyangah, C. Jaebum, J.I. Hong, A.J.D. Mello, Surface-enhanced Raman scattering in nanoliter droplets: towards high-sensitivity detection of mercury (II) ions, Analytical & Bioanalytical Chemistry, 394 (2009) 1827-1832.

[25] Y. Chen, L. Wu, Y. Chen, N. Bi, X. Zheng, H. Qi, M. Qin, X. Liao, H. Zhang, Y. Tian, Determination of mercury(II) by surface-enhanced Raman scattering spectroscopy based on thiol-functionalized silver nanoparticles, Microchimica Acta,

177 (2012) 341-348.

[26] C. Gao, X.J. Huang, Voltammetric determination of mercury(II), Trac Trends in Analytical Chemistry, 51 (2013) 1-12.

[27] D. Martín-Yerga, M.B. González-García, A. Costa-García, Electrochemical determination of mercury: A review, Talanta, 116 (2013) 1091-1104.

[28] X. Zhu, B. Liu, H. Hou, Z. Huang, K.M. Zeinu, L. Huang, X. Yuan, D. Guo, J. Hu, J. Yang, Alkaline intercalation of Ti3C2 MXene for simultaneous electrochemical detection of Cd(II), Pb(II), Cu(II) and Hg(II), Electrochim Acta, 248 (2017) 46-57.

[29] C.W. Liu, C.C. Huang, H.T. Chang, A. Chem, Highly selective DNA-based sensor for lead(II) and mercury(II) ions, Anal Chem, 81 (2009) 2383-2387.

[30] A.C. Girvan, Y. Teng, L.K. Casson, S.D. Thomas, S. Jüliger, M.W. Ball, J.B. Klein, P.W. Jr, S.S. Barve, P.J. Bates, AGRO100 inhibits activation of nuclear factor-kappaB (NF-kappaB) by forming a complex with NF-kappaB essential modulator (NEMO) and nucleolin, Mol Cancer Ther, 5 (2006) 1790.

[31] L. Song, X. Pan, H. Shen, Y. Yu, Microflow injection potassium bioassay based on G-quadruplex DNAzyme-enhanced chemiluminescence, Luminescence, 29 (2015) 1066-1073.

[32] Y. Zhang, B. Li, Reducing background signal of G-quadruplex-hemin DNAzyme sensing platform by single-walled carbon nanotubes, Biosens Bioelectron, 27 (2011) 137-140.

[33] N. Smargiasso, F. Rosu, H. Wei, P. Colson, E.S. Baker, M.T. Bowers, E.D. Pauw, V. Gabelica, G-Quadruplex DNA Assemblies: Loop Length, Cation Identity, and

Multimer Formation, J Am Chem Soc, 130 (2008) 10208-10216.

[34] J. Kypr, I. Kejnovska, D. Renciuk, M. Vorlickova, Circular dichroism and conformational polymorphism of DNA, Nucleic Acids Res, 37 (2009) 1713.

[35] A. Bourdoncle, A. Estévez Torres, C. Gosse, L. Lacroix, P. Vekhoff, T. Le Saux, L. Jullien, and, J.L. Mergny, Quadruplex-Based Molecular Beacons as Tunable DNA Probes, J Am Chem Soc, 128 (2006) 11094-11105.

[36] A. Guédin, C.A. De, J. Gros, L. Lacroix, J.L. Mergny, Sequence effects in single-base loops for quadruplexes, Biochimie, 90 (2008) 686-696.

[37] A. Bugaut, S. Balasubramanian, A sequence-independent study of the influence of short loop lengths on the stability and topology of intramolecular DNA G-quadruplexes, Biochemistry, 47 (2008) 689-697.

[38] L.A. Marky, K.J. Breslauer, Calculating thermodynamic data for transitions of any molecularity from equilibrium melting curves, Biopolymers, 26 (1987) 1601.

[39] WHO, Guidelines for drinking-water quality - 4th edition, (2011).

[40] D. Li, A. Wieckowska, I. Willner, Optical Analysis of Hg2+ Ions by Oligonucleotide–Gold-Nanoparticle Hybrids and DNA-Based Machines, Angewandte Chemie, 47 (2008) 3927.

[41] E. Norkus, I. Stalnionien, D.C. Crans, Interaction of pyridine- and 4-hydroxypyridine-2,6-dicarboxylic acids with heavy metal ions in aqueous solutions, Heteroatom Chemistry, 14 (2003) 625–632.